Gyrokinetic modeling: A multi-water-bag approach

P. Morel, E. Gravier, N. Besse, R. Klein, A. Ghizzo, and P. Bertrand
Laboratoire PMIA, UMR 7040 CNRS-Université Henri Poincaré, F-54506 Vandoeuvre-lès-Nancy Cedex, France

X. Garbet, P. Ghendrih, V. Grandgirard, and Y. Sarazin
CEA/DSM/Département de Recherche sur la Fusion Contrôlée, Association Euratom-CEA, Cadarache, 13108 St Paul-lez-Durance, France

(Received 30 March 2007; accepted 2 October 2007; published online 29 November 2007)

Predicting turbulent transport in nearly collisionless fusion plasmas requires one to solve kinetic (or, more precisely, *gyrokinetic*) equations. In spite of considerable progress, several pending issues remain; although more accurate, the kinetic calculation of turbulent transport is much more demanding in computer resources than fluid simulations. An alternative approach is based on a water-bag representation of the distribution function that is not an approximation but rather a special class of initial conditions, allowing one to reduce the full kinetic Vlasov equation into a set of hydrodynamic equations while keeping its kinetic character. The main result for the water-bag model is a lower cost in the parallel velocity direction since no differential operator associated with some approximate numerical scheme has to be carried out on this variable $v_{\|}$. Indeed, a small bag number is sufficient to correctly describe the ion temperature gradient instability. © *2007 American Institute of Physics*. [DOI: 10.1063/1.2804079]

I. INTRODUCTION

Microinstabilities are now commonly held responsible for turbulence giving rise to anomalous radial energy transport in tokamak plasmas. Such a turbulent transport governs the energy confinement time in controlled fusion devices. In this framework, the quest for performant discharges with good confinement properties relies crucially on our ability to accurately predict the level of turbulent transport. The low frequency ion-temperature-gradient-driven (ITG) turbulence is one of the most serious candidates to account for this anomalous transport,[1] as well as the so-called trapped electron modes.[2] During recent years, ion turbulence in tokamaks has been studied intensively both with fluid (see, for instance, Refs. 3–5) and gyrokinetic simulations using particle-in-cell codes[6–8] or Vlasov codes.[9–12]

It is now well known that the kinetic and fluid descriptions of the instability can lead to different linear properties; namely, the instability threshold and the linear growth rate.[13–15] Besides, fluid codes are usually reported to overestimate the turbulent transport level.[16] So as to reduce the discrepancies between these two approaches, new fluid closures have been recently developed to account for some kinetic effects.[17–21] In this framework, it is important that gyrokinetic simulations quantify the departure of the local distribution function from a Maxwellian, which constitutes the usual assumption of fluid closures.

In a recent paper,[22] a comparison between fluid and kinetic approach has been addressed by studying a three-dimensional kinetic interchange. A simple drift-kinetic model is described by a distribution depending on only two spatial dimensions and parametrized by the energy. In that case it appears that the distribution function is far from a Maxwellian and cannot be described by a small number of moments. Wave-particle resonant processes certainly play an important role and most of the closures that have been developed will be inefficient.

On the other hand, although more accurate, the kinetic calculation of turbulent transport is much more demanding in computer resources than fluid simulations. This motivated us to revisit an alternative approach based on the water-bag (WB) representation.

Introduced initially by DePackh,[23] Hohl, Feix, and Bertrand[24–26] the water-bag model was shown to create a bridge between fluid and kinetic descriptions of a collisionless plasma. Furthermore, this model was extended to a double water bag by Berk and Roberts[27] and Finzi,[28] and was further generalized to the multiple water bag.[30–33]

It is the aim of this paper to revisit this model and its possible application to gyrokinetic modeling.

After a brief introduction of the well known gyrokinetic context, we will present the water-bag model, stressing the reasons that it is well suited in a gyro context. A linear analysis of the slab branch of ITG modes using the water-bag distribution will be presented. Finally, the first attempts to developing nonlinear numerical simulations will be discussed.

II. THE WATER BAG MODEL FOR GYROKINETIC MODELING

A. The drift-kinetic equation

Although the gyrokinetic reduction from Hamiltonian consideration can be carried on in different phase space coordinates such as action-angle variables, as done in Ref. 9, the usual gyrokinetic description as used for instance in the GYSELA code (as described in Ref. 10) makes full use of the $v_{\|}, \mu$ coordinates: the $v_{\|}$ variable is indeed a kinetic variable, while the μ (magnetic moment) is a *label* associated with a

set of distribution functions f_μ. In the more simple drift-kinetic description, only $\mu=0$ is considered.

The ITG instability relies on the resonant interaction between waves and particles. In principle, one has to solve a six-dimensional kinetic equation to determine the distribution function. However, for strongly magnetized plasmas, the Larmor radius r_L is much smaller than the characteristic length L of density or magnetic field, and the cyclotron motion is faster than the turbulent motion. The Vlasov equation can then be expanded in r_L/L and averaged over the cyclotron motion. The new equation is called the drift-kinetic equation. It is also possible to take into account finite Larmor radius effects by adding gyroaveraging and polarization drift into the drift-kinetic equation, leading to the gyrokinetic model.[34] Thus, for strongly magnetized plasmas, gyrokinetics allows us to recast the Vlasov equation into a five-dimensional equation in which the fast gyroangle does not appear explicitly, but in which the particle information is not lost.

The gyrokinetic model is based on the Vlasov equation for the guiding-center ion distribution function $f=f(\mathbf{r},v_\parallel,t)$. With an adiabatic response for the electrons,[34] we get

$$\partial_t f + \mathbf{v_E}\,.\,\boldsymbol{\nabla} f + \mathbf{v}_g\,.\,\boldsymbol{\nabla} f + v_\parallel \boldsymbol{\nabla}_\parallel f + \dot{v}_\parallel \partial_{v_\parallel} f = 0, \tag{1}$$

where

$$\mathbf{v_E} = \frac{\mathbf{B}}{B} \times \frac{\boldsymbol{\nabla} \mathcal{J}_0 \phi}{B}, \tag{2}$$

$$\mathbf{v}_g = \frac{M_i v_\parallel^2}{q_i B}\left(\frac{\mathbf{B}}{B} \times \frac{\mathbf{N}}{R_c}\right) + \frac{\mu}{q_i}\left(\frac{\mathbf{B}}{B} \times \frac{\boldsymbol{\nabla} \mathbf{B}}{B}\right), \tag{3}$$

$$\dot{v}_\parallel = -\left[\frac{\mathbf{B}}{B} + \frac{M_i v_\parallel^2}{q_i B}\left(\frac{\mathbf{B}}{B} \times \frac{\mathbf{N}}{R_c}\right)\right] . \left[\frac{\mu}{M_i} \boldsymbol{\nabla} \mathbf{B} + \frac{q_i}{M_i} \boldsymbol{\nabla} \mathcal{J}_0 \phi\right], \tag{4}$$

and where $\mathcal{J}_0$ is the gyroaverage operator, $\mathbf{N}/R_c$ is the field line curvature, and μ is the first adiabatic invariant of the ion gyrocenters. The quasineutrality equation reads

$$Z_i \mathcal{J}_0 n_i + Z_i \frac{q_i}{T_i} r_L^2 \boldsymbol{\nabla}_\perp (n_i \boldsymbol{\nabla}_\perp \phi) = n_{e0} e^{e(\phi - \langle \phi \rangle_\parallel)/T_e}. \tag{5}$$

The second term on the left-hand side of this equation corresponds to the polarization density. Moreover, to study slab ion temperature gradients instabilities, a simplified drift-kinetic model in cylindrical geometry[10] is used in this paper:

- The uniform and constant magnetic field $\mathbf{B}$ is along the axis of the column (z coordinate). It follows the perpendicular drift velocity does not admit any magnetic curvature or gradient effect: $\mathbf{v}_g=\mathbf{0}$ and $\mathbf{v}_\perp=\mathbf{v}_E=\mathbf{E}\times\mathbf{B}/B^2$.
- The equation of motion provides $\dot{v}_\parallel=q_iE_\parallel/M_i$.
- Ion finite Larmor radius effects are neglected as well so that only the guiding-center trajectories are taken into account: $\mathcal{J}_0=1$, $k_\perp r_L \to 0$, where r_L is the ion Larmor radius.
- Electron inertia is ignored (adiabatic response to the low frequency fluctuations), electric potential is small when compared to the electron kinetic energy: $e\phi \ll T_e$.

There is no equilibrium radial electric field. The plasma quasineutrality approximation $\delta n_i = \delta n_e$ is sufficient for low frequency electrostatic perturbations.

With these assumptions, the evolution of the ion guiding-center distribution function $f(\mathbf{r}_\perp,z,v_\parallel,t)$ is described by the drift-kinetic Vlasov equation (see Ref. 10 for more details)

$$\partial_t f(\mathbf{r},v_\parallel,t) + \mathbf{v_E} \cdot \boldsymbol{\nabla}_\perp f(\mathbf{r},v_\parallel,t) + v_\parallel \partial_z f(\mathbf{r},v_\parallel,t) + \frac{q_i E_\parallel}{M_i} \partial_{v_\parallel} f(\mathbf{r},v_\parallel,t) = 0 \tag{6}$$

for the ions (q_i,M_i), coupled to an adiabatic electron response via the quasineutrality assumption

$$Z_i \int_{-\infty}^{+\infty} f(\mathbf{r},v_\parallel,t) dv_\parallel = n_{e0}\left(1 + \frac{e\phi}{T_e}\right) \tag{7}$$

assuming $(e\phi \ll T_e)$. Here, $e=+1.6\times10^{-19}$ C, $q_i=Z_ie$, and $\mathbf{v_E}$ is the $E\times B$ drift velocity.

The most important and interesting feature is that f *depends only on the velocity component* $v_\parallel$ parallel to $\mathbf{B}$. Let us now turn to the *water-bag* model.

B. The water-bag model

Consider a more simple problem, in which the physical quantities do not depend on the perpendicular direction $\mathbf{r}_\perp$ [i.e., two-dimensional (2-D) phase space $z,v_\parallel$], in which at initial time the situation is depicted as follows.

Consider two single-valued functions $v_+(z)>v_-(z)$ in phase space. Between the two corresponding curves, we impose $f(z,v_\parallel,0)=A$ (A is a constant). For velocities bigger than v_+ and smaller than v_-, we have $f(z,v_\parallel,0)=0$.

According to phase space conservation property of the Vlasov equation, as long as v_+ and v_- remain single-valued functions, $f(z,v_\parallel,t)$ remains equal to A for values of $v_\parallel$ such that $v_-(x,t)<v_\parallel<v_+(x,t)$. Therefore, the problem is entirely described by the two functions $v_+(z,t)$ and $v_-(z,t)$.

Remembering that a particle on the contour v_+ (or v_-) remains on this contour, the equations for v_+ and v_- are

$$\frac{Dv_\pm}{Dt} = \frac{\partial v_\pm(z,t)}{\partial t} + v_\pm \frac{\partial v_\pm}{\partial z} = \frac{q_i}{M_i} E_\parallel(z,t). \tag{8}$$

Now let us introduce the density $n(x,t)=A(v_+-v_-)$ and the average (fluid) velocity $u(x,t)=\frac{1}{2}(v_++v_-)$ into Eqs. (8) by adding and subtracting these two equations. We obtain

$$\frac{\partial n}{\partial t} + \frac{\partial}{\partial z}(nu) = 0, \tag{9}$$

$$\frac{\partial u}{\partial t} + u\frac{\partial u}{\partial z} = -\frac{1}{M_i n}\frac{\partial P}{\partial z} + \frac{q_i}{M_i} E_\parallel(z,t) \tag{10}$$

$$Pn^{-3} = \frac{M_i}{12A^2}. \tag{11}$$

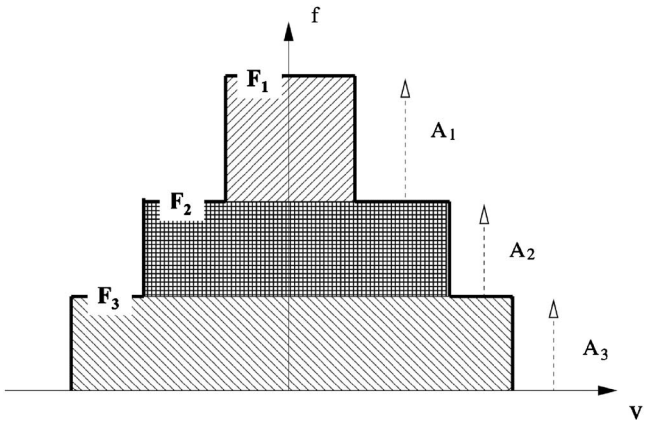

FIG. 1. The multi-water-bag distribution function along the velocity direction ($v_\parallel$).

Equations (9)–(11) are, respectively, the continuity, Euler, and state equations. This hydrodynamic description of the water-bag model was pointed out for the first time by Bertrand and Feix,[25] but the state equation (11) describes an invariant both in space and time while in the hydrodynamic model we obtain $(D/Dt)(Pn^{-\gamma})=0$. It must be noticed that the physics in the two cases is quite different.[35]

The generalization to the *multiple-water-bag model* was straightforward;[30–32] Berk and Roberts[27] and Finzi[28] used a double WB model to study the two-stream instability in a computer simulation including the filamentation of the contours and their multivalued nature (a highly difficult problem from a programming point of view).

Let us consider $2N$ contours in phase space labeled v_j^+ and v_j^- (where $j=1,\ldots,N$). Figure 1 shows a three-bag system ($N=3$) where the distribution function takes on three different constant values: F_1, F_2, and F_3.

Introducing the *bag* heights A_1, A_2, and A_3, as shown also in Fig. 2, the distribution function reads

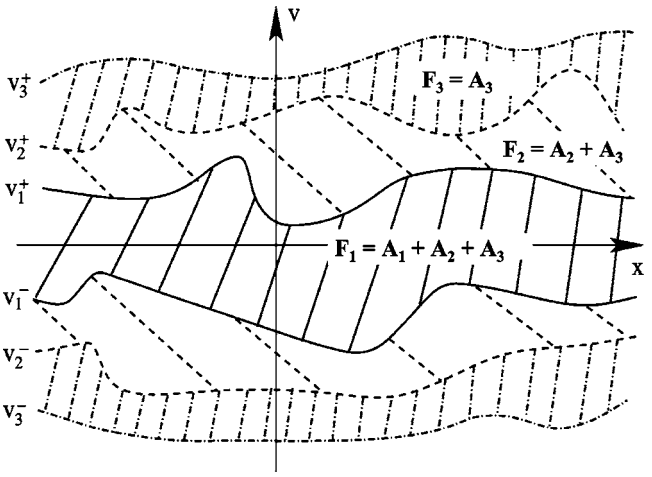

FIG. 2. Contours $v_j^\pm$ in the phase space $(z,v_\parallel)$ for a three-bag system, and associated values of the distribution function.

$$f(z,v_\parallel,t)=\sum_{j=1}^{N} A_j\{\Upsilon[v_\parallel-v_j^-(z,t)]-\Upsilon[v_\parallel-v_j^+(z,t)]\}, \quad (12)$$

where Υ is the Heaviside unit step function. Notice that some of the A_j can be negative. With respect to the conservation property of the Vlasov equation, the height A_j of each bag is a constant of the motion (see Fig. 1).

The properties of the system are completely described by the knowledge of the contours $v_j^\pm$, which obey the motion equations

$$\frac{Dv_j^\pm}{Dt}=\frac{\partial v_j^\pm(z,t)}{\partial t}+v_j^\pm\frac{\partial v_j^\pm}{\partial z}=\frac{q_i}{M_i}E_\parallel(z,t). \quad (13)$$

Let us now introduce for each bag j the density n_j, average velocity u_j, and pressure P_j, as done above for the one-bag case: $n_j=A_j(v_j^+-v_j^-)$, $u_j=(1/2)(v_j^++v_j^-)$, and $P_jn_j^{-3}=M_i/(12A_j^2)$. For each bag j, we recover the continuity and Euler equations as written in Eqs. (9) and (10); namely,

$$\frac{\partial n_j}{\partial t}+\frac{\partial}{\partial z}(n_ju_j)=0, \quad (14)$$

$$\frac{\partial u_j}{\partial t}+u_j\frac{\partial u_j}{\partial z}=-\frac{1}{M_in_j}\frac{\partial P_j}{\partial z}+\frac{q_i}{M_i}E_\parallel(z,t). \quad (15)$$

The coupling between the bags is given by the total density $\Sigma_j n_j$ in the quasineutrality equation.

C. Water-bag model and moments of a continuous distribution function

The connection with a multifluid model is more illuminating if we consider the equivalence *in the fluid momentum sense* of a multi-water-bag distribution and a continuous distribution.[40]

Let us consider an homogeneous equilibrium distribution function $f_0(v_\parallel)$. For simplicity, we suppose f_0 is an even function of $v_\parallel$ (odd momenta are zero). In the water-bag formalism, this means symmetrical equilibrium contours $v_j^\pm=\pm a_j$. Let us define the ℓ-momentum of f_0 (ℓ even only) as

$$\mathcal{M}_\ell(f_0)=\int_{-\infty}^{\infty} v_\parallel^\ell f_0(v_\parallel)dv_\parallel \quad (16)$$

and the ℓ-momentum of the corresponding water bag as

$$\mathcal{M}_\ell(\mathrm{WB})=\frac{1}{\ell+1}\sum_j 2A_ja_j^{\ell+1}. \quad (17)$$

Let us now sample the $v_\parallel$ axis with appropriate a_j values. Thus, equating Eqs. (16) and (17) for $\ell=0,2,\ldots,2(N-1)$ yields a system of N linear equations for the N unknown A_j, $j=1,\ldots,N$. Using an integration by parts, we get

$$\sum_j 2A_ja_j^{\ell+1}=-\int_{-\infty}^{\infty} v_\parallel^{\ell+1}\frac{df_0}{dv_\parallel}dv_\parallel, \quad \ell=0,2,\ldots,2(N-1). \quad (18)$$

A water-bag model with N bags is equivalent to a continuous distribution function for momenta up to $\ell_{\max}=2(N-1)$. Nevertheless, Eq. (18) has the form of a Vandermonde

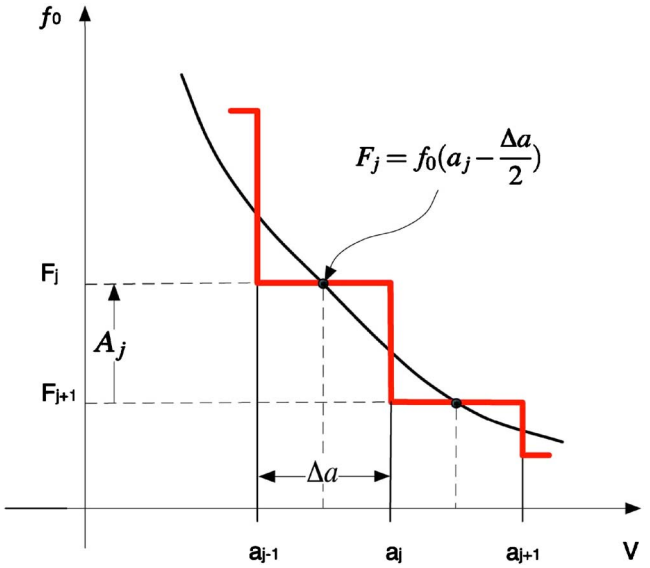

FIG. 3. (Color online) Distribution of the initial bag velocities a_j and associated values of F_j.

system that becomes ill-conditioned for higher values of the number of bags N (for instance, for $N=15$ and a cutoff in velocity space $a_N=5v_{Ti}$ the matrix elements vary from 1 to 5^{28}).

A more convenient solution can be found for a larger number of bags and for a regular sampling of the $v_\parallel$ axis; i.e., $a_j=(j-1/2)\Delta a$ (see Fig. 3). The idea is to compute the F_j values at the middle of each interval $\Delta a=a_N/(N-1/2)$; we have $F_j=f_0(a_j-\Delta a/2)$ and $F_{j+1}=f_0(a_j+\Delta a/2)$. With such a choice of a_j distribution and since $A_j=F_j-F_{j+1}$, from Eq. (18) the solution is straightforward:

$$\frac{-A_j}{\Delta a} = \frac{df_0}{dv_\parallel} + \mathcal{O}(\Delta a^2). \tag{19}$$

As depicted in Fig. 4, such an approximation becomes accurate for N greater than 10. Of course, for N smaller than 10, the exact A_j can be obtained solving directly the linear system (18).

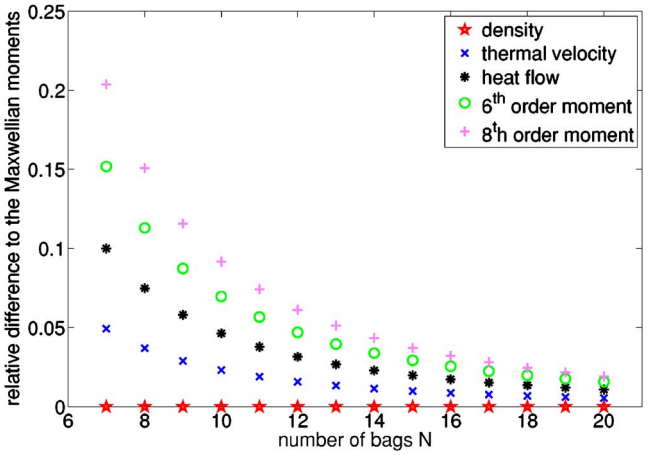

FIG. 4. (Color online) Accuracy of the second-order Taylor expansion method when compared with a continuous Maxwellian distribution function, as a function of the number of bags (N).

D. Using water-bag invariants to reduce phase space dimension

In Eq. (13), j is nothing but a *label* since *no* differential operation is carried out on the variable $v_\parallel$. What we actually do is to bunch together particles within the same bag j and let each bag evolve using the contour equations (13). Of course, the different bags are coupled through Poisson's equation.

This operation appears as an *exact* reduction of the phase space dimension (elimination of the velocity variable) in the sense that the water-bag concept makes full use of the Liouville invariance in phase space: the fact that the A_j are constant in time is nothing but a straightforward consequence of the Vlasov conservation $Df/Dt=0$. Of course, the eliminated velocity reappears in the various bags j $(j=1,\ldots,N)$, and if we need a precise description of a continuous distribution a large N is needed. On the other hand, there is no mathematical lower bound on N and from a physical point of view, many interesting results can even be obtained with N as small as 1 for an electrostatic plasma. For magnetized plasma, $N=2$ or 3 allow more analytical approaches (as seen below).

On the contrary, in the Vlasov phase space $(z,v_\parallel)$, the exchange of velocity is described by a differential operator. From a numerical point of view, this operator has to be *approximated* by some finite difference scheme. Consequently, a minimum size for the mesh in the velocity space is required and we are faced with the usual sampling problem: If it can be claimed that the $v_\parallel$-gradients of the distribution function remain weak enough for some class of problems, then a rough sampling might be acceptable.[41] However, it is well known in kinetic theory that wave-particle interaction is often not so obvious. For instance, steep gradients in velocity space can be the signature of strong wave-particle interaction and there is the need for a higher numerical resolution of the Vlasov code, while a water-bag description can still be used with a small bag number. As a matter of fact, it is well known that this mesh problem is closely related to poor entropy conservation (see, for instance, Ref. 29).

To conclude, the multiple water bag offers an exact description of the plasma dynamics even with a small bag number, allowing more analytical studies and bringing the link between the hydrodynamic description and the full Vlasov one. Of course this needs a special initial preparation of the plasma. Moreover, if we need a precise description of a continuous distribution, it is clear that a larger N is needed; but even if the numerical effort is close to a standard discretization of the velocity space in a regular Vlasov code (using $2N+1$ mesh points), we believe that the use of an exact water-bag sampling should give better results than approximating the corresponding differential operator.

E. The gyro water-bag (GWB) model

Let us now turn back to the drift-kinetic equation (6). Since the distribution $f(\mathbf{r}_\perp,z,v_\parallel,t)$ takes into account only one velocity component $v_\parallel$, a water bag can be considered and Eq. (12) now reads

$$f(\mathbf{r}_\perp,z,v_\parallel,t)=\sum_{j=1}^{N}A_j\{\Upsilon[v_\parallel-v_j^-(\mathbf{r}_\perp,z,t)]-\Upsilon[v_\parallel-v_j^+(\mathbf{r}_\perp,z,t)]\},\tag{20}$$

and provides the set of contour equations

$$\partial_t v_j^\pm+\mathbf{v_E}\cdot\boldsymbol{\nabla}_\perp v_j^\pm+v_j^\pm\partial_z v_j^\pm=\frac{q_iE_\parallel}{M_i}\tag{21}$$

coupled to the multi-water-bag quasineutrality

$$Z_i\sum_{j=1}^{N}A_j(v_j^+-v_j^-)=n_{e0}\left(1+\frac{e\phi}{T_e}\right).\tag{22}$$

Let us introduce for each bag j the density $n_j=(v_j^+-v_j^-)A_j$ and the average velocity $u_j=(v_j^++v_j^-)/2$. Equations (21) and (22) allow us to recover continuity and Euler equations; namely,

$$\frac{\partial n_j}{\partial t}+\boldsymbol{\nabla}_\perp\cdot(n_j\mathbf{v_E})+\partial_z(n_ju_j)=0,\tag{23}$$

$$\frac{\partial u_j}{\partial t}+\mathbf{v_E}\cdot\boldsymbol{\nabla}_\perp u_j+u_j\frac{\partial u_j}{\partial z}=-\frac{1}{M_in_j}\frac{\partial P_j}{\partial z}+\frac{q_i}{M_i}E_\parallel,\tag{24}$$

where M_i and q_i are ion mass and charge, respectively.

The partial pressure takes the form

$$P_j=M_in_j^3/(12A_j^2).\tag{25}$$

The connection between kinetic and fluid description clearly appears in the previous equations: the case of one bag recovers a fluid description (with an exact closure) and the limit of an infinite number of bags provides a continuous distribution function.

III. LINEAR ANALYSIS AND GYRO WATER-BAG DISPERSION RELATION

A direct illustration of GWB's ability to reproduce the physical features of gyrokinetics is given by the linear analysis of the gyro water-bag equations (21) and (22). On the following pages an even equilibrium multi-water-bag distribution $v_j^\pm=\pm a_j(r)$ depending only on the radial variable r will be assumed.

A. Linearizing the gyro water-bag equations

Let us consider the following expansion around the equilibrium:

$$v_j^\pm(r,\theta,z,t)=\pm a_j(r)+w_j^\pm(r)e^{i(m\theta+k_\parallel z-\omega t)}+\text{c.c.},\tag{26}$$

$$\phi(r,\theta,z,t)=0+\delta\phi(r)e^{i(m\theta+k_\parallel z-\omega t)}+\text{c.c.}\tag{27}$$

assuming that plane wave dependencies are convenient with a linear analysis. Defining $k_\theta=m/r$, we obtain the linear water-bag system

$$(\omega\mp k_\parallel a_j)w_j^\pm-\left[\frac{q_ik_\parallel}{M_i}\mp\frac{k_\theta}{B}\right]\delta\phi=0,\tag{28}$$

$$Z_i\sum_{j=1}^{N}A_j(w_j^+-w_j^-)=\frac{en_{e0}}{T_e}\delta\phi,\tag{29}$$

from which the multi-water-bag dispersion relation $\epsilon_{\hat{k}_\theta}(\hat{\omega})=0$ is easily obtained. The gyro water-bag dispersion function is written in normalized units,

$$\epsilon_{\hat{k}_\theta}(\hat{\omega})=1-Z_i^\star\sum_{j=1}^{N}\alpha_j\frac{1-\hat{\omega}\hat{\Omega}_j^\star}{\hat{\omega}^2-\hat{a}_j^2},\tag{30}$$

where $Z_i^\star=Z_iT_e/T_i$. The normalizations are defined as follows (by using $v_{Ti}^2=T_i/M_i$):

$$\hat{\omega}=\omega/k_\parallel v_{Ti},\tag{31}$$

$$\hat{a}=a/v_{Ti},\tag{32}$$

$$\hat{k}=k/k_\parallel,\tag{33}$$

$$\hat{\phi}=q_i\phi/T_i.\tag{34}$$

Moreover, two water-bag parameters have been introduced in Eq. (30):

- The relative bag density $\alpha_j=2A_ja_j/n_{i0}$ [where $n_{i0}(r)$ is the radial ion density profile].
- The water-bag diamagnetic frequency related to bag j: $\hat{\Omega}_j^\star=\hat{k}_\theta d_r\ln(a_j)/\hat{\Omega}_{Ci}$, where $\hat{\Omega}_{Ci}=q_iB/(M_ik_\parallel v_{Ti})$. It is interesting to note that $\Omega_j^\star$ values are related to the diamagnetic frequency $\Omega_n^\star$ by the relation $\Sigma_{j=1}^N\alpha_j\Omega_j^\star=\Omega_n^\star$.

For simplicity, the $\hat{\cdot}$ notation will be dropped on the following pages.

B. Water-bag and Landau damping of ion acoustic waves

The special case without radial dependence [i.e., $a_j(r)=\text{const}$ or $\Omega_j^\star=0$] will be interesting to consider first. It will help us to understand how kinetic effects will be taken into account with the water-bag model and more precisely how the linear Landau damping can be recovered for ion acoustic waves as a phase mixing process of undamped eigenmodes,[30,33] which is reminiscent of the Van Kampen–Case treatment of the electronic plasma oscillations.[36,37]

Setting $\Omega_j^\star=0,\ \forall\ j=1,\ldots,N$ in Eq. (30), the dielectric plasma function becomes an even function of ω:

$$\epsilon(\omega)=1-Z_i^\star\sum_{j=1}^{N}\frac{\alpha_j}{\omega^2-a_j^2}.\tag{35}$$

The one-bag case allows us to recover the usual acoustic frequency:

$$\omega^2=(3+Z_i^\star).\tag{36}$$

Now, if all A_j are positive (single-hump distribution function), Eq. (35) has $2N$ real frequencies $\pm\omega_n$ located between $\pm a_j$ and $\pm a_{j+1}$ (see Fig. 5).

The water-bag description is a discrete form of the continuous spectral Van Kampen–Case approach.[36,37] The resulting time-dependent electric potential is obtained by solving

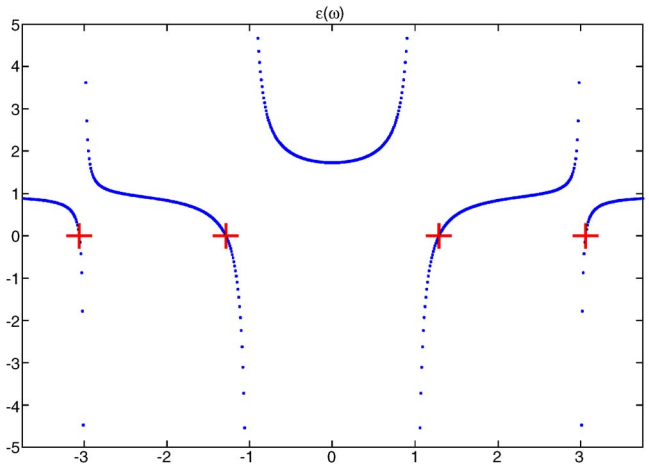

FIG. 5. (Color online) Dependency of the plasma dielectric function on ω for a two-bag case. Zeros are represented with a + sign. $N=2$, $Z_i^\star=1$.

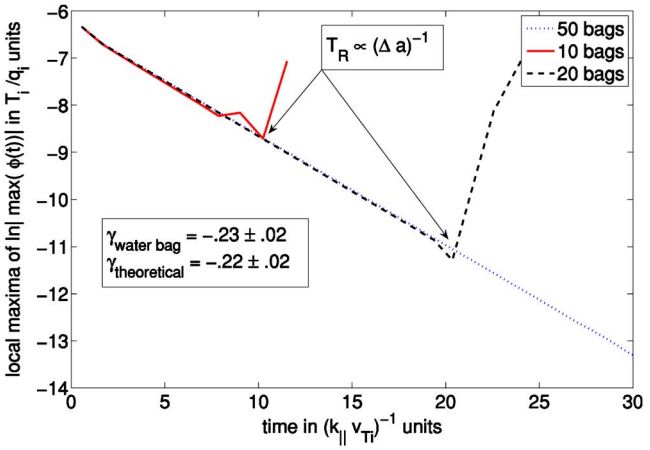

FIG. 6. (Color online) Linear Landau damping: time evolution of the electric potential (normalized units) with $Z_i^\star=5$.

the linear water-bag system as an eigenvalue problem. The eigenfunctions $W_j=A_j w_j$ obey the eigenvalue equation

$$(\omega_n - a_j)W_j - Z_i^\star \frac{\alpha_j}{2a_j} \sum_{\substack{k=-N \\ k\neq 0}}^{N} W_k = 0, \quad k \neq 0, \tag{37}$$

assuming the electric potential can be written

$$\phi(z,t) = \sum_{j=1}^{N} C_n e^{i(k_\parallel z - \omega_n t)}. \tag{38}$$

The coefficient C_n values are given by

$$C_n = \frac{\Sigma_{j=1}^{N}[\omega_n(\varepsilon_j^{0+} - \varepsilon_j^{0-}) + a_j(\varepsilon_j^{0+} + \varepsilon_j^{0-})]/(\omega_n^2 - a_j^2)}{\Sigma_{j=1}^{N} 2\omega_n \alpha_j/(\omega_n^2 - a_j^2)^2}, \tag{39}$$

where the quantities $\varepsilon_j^{0\pm}$ are the relative amplitude of the initial contour perturbation

$$v_j^{\pm}(z, t=0) = \pm a_j(1 + \varepsilon_j^{0\pm} e^{ik_\parallel z} + \text{c.c.}).$$

The electric potential [Eq. (38)] behaves like a superposition of N oscillators that are in phase at time 0. As time increases they will gradually lose their synchronization and the electric potential decreases according to the Landau prediction (see Fig. 6). In the case of a Maxwellian equilibrium distribution function the theoretical damping rate is given by the imaginary part of solutions of the following equation:

$$1 - 2Z_i^\star \frac{d\mathcal{Z}(\omega)}{d\omega} = 0, \tag{40}$$

where $\mathcal{Z}$ is the well known Fried-Conte function. For example, for $Z_i^\star=5$, the water-bag value $\gamma_{\text{WB}}=-0.23\pm0.02$ is very close to the theoretical value $\gamma_{\text{theoretical}}=-0.22\pm0.02$.[38]

It should be pointed out that a recurrence phenomenon is occurring in Fig. 6. The recurrence time T_R is related to the possibility for the N oscillators to return almost in phase after a time of the order of the longest period (corresponding to the smallest pulsation value). This recurrence time T_R is

$$T_R \sim \frac{2\pi}{\Delta a}.$$

This recurrence is a well known phenomenon in Vlasov simulations for situations close to linear ones, where the field is small. The free streaming of particles gives rise to a fine structure in velocity space: if the free streaming is the only process ($\mathbf{E}=\mathbf{0}$), the exact solution of the Vlasov equation $(\partial f/\partial t + v\partial f/\partial x = 0)$ is $f_k(v,t)=f_0(v)\exp(ikvt)$; if a numerical discretization is introduced with a mesh size Δv, it is clear that a recurrence effect has to occur at time $T_R=2\pi/k\Delta v$. Of course, it is the same for the water bag with its natural (not numerical) discretization of the velocity space. Actually, this recurrence phenomenon disappears when the nonlinearity is more important and hides the free streaming.[39]

IV. THE ITG INSTABILITY

The aim of the present section is to complete a linear analysis of drift-kinetic water-bag equations, in order to compare our model to analytical results obtained with continuous Maxwellian distribution function. Such an analysis will provide a test for the nonlinear solver, which will be presented in the last part of the paper and in a forthcoming paper.

A. Radial multi-water-bag parameters and moments of a continuous distribution function

The first problem we have to solve is to determine physically relevant radial water-bag parameter. We use the same method as given in Sec. II C, by considering both momenta and their radial derivatives. With a view to describe ITG modes, we choose to develop radial profiles in terms of temperature and density profiles only.

The continuous distribution function is assumed as follows:

$$f_{\text{eq}}(\mathbf{r}, v_\parallel) = \frac{n_{i0}}{v_{Ti}} \mathcal{G}\left(\frac{v_\parallel}{v_{Ti}}\right), \tag{41}$$

where $\mathcal{G}$ is a normalized and even function. $n_{i0}(r)$ and $v_{Ti}(r)$ are the radial profiles of ion density and thermal velocity, respectively.

Consider now the gyro water-bag dispersion function (30). *At a given point* $r=r_0$ the α_j can be computed using the

same trick as explained in Sec. II C. However, as compared to Eq. (35), new unknown $\Omega_j^\star$ appear that measure the local density gradient of the corresponding bag j. Of course, these unknowns have a sense relative to our model. They have to be calculated from the knowledge of the *equilibrium gradients at* $r=r_0$; namely, the diamagnetic frequencies expressed in terms of the density gradient $\Omega_n^\star$ and the temperature gradient $\Omega_T^\star$. Let us write

$$\alpha_j \Omega_j^\star = \tfrac{1}{2}\beta_j \Omega_T^\star + \gamma_j \Omega_n^\star, \tag{42}$$

where the unknown coefficients β_j and γ_j are determined as follows. In Sec. II C, a method was given to compute the α_j from an equivalence between the moments of the stepwise water bag and the corresponding continuous function. Taking the derivative of the moments along radial direction, and using Eq. (41), we obtain

$$\sum_{j=1}^{N} \alpha_j \Omega_j^\star a_j^l = \left(\Omega_T^\star \frac{l}{2} + \Omega_n^\star\right) v_{Ti}^l \mathcal{M}_l, \tag{43}$$

where $\mathcal{M}_l$ is the lth-order moment of the $\mathcal{G}$ function, with the definition

$$\mathcal{M}_l = \int_{-\infty}^{+\infty} x^l \mathcal{G}(x) dx, \quad l = 0, 2, \ldots, 2(N-1). \tag{44}$$

Finally, inserting expression (42) in Eq. (43), and separating between $\Omega_T^\star$ and $\Omega_n^\star$, yields the coefficients for each bag:

$$\sum_{j=1} \alpha_j a_j^l = (l+1) v_{Ti}^l \mathcal{M}_l, \tag{45}$$

$$\sum_{j=1} \beta_j a_j^l = l v_{Ti}^l \mathcal{M}_l, \tag{46}$$

$$\sum_{j=1} \gamma_j a_j^l = v_{Ti}^l \mathcal{M}_l. \tag{47}$$

In Eqs. (45)–(47), the matrix we have to invert remains a Vandermonde one, with the same numerical problem as in Sec. II C. A Taylor expansion provides us

$$\alpha_j = 2a_j \frac{F_j - F_{j+1}}{n_{i0}}, \tag{48}$$

$$\gamma_j = \Delta a \frac{F_j + F_{j+1}}{n_{i0}}, \tag{49}$$

$$\beta_j = \alpha_j - \gamma_j. \tag{50}$$

It is important to note that we have supposed a relatively general form of the distribution function (41), including the case of non-Maxwellian equilibrium distribution functions.

B. Instability threshold and linear growth rate

With respect to radial dependencies $(\Omega_T^\star, \Omega_n^\star)$, the dielectric plasma function (30) could now admit complex conjugate roots corresponding to reversing some asymptotes. Finding the instability threshold is equivalent to solving the system

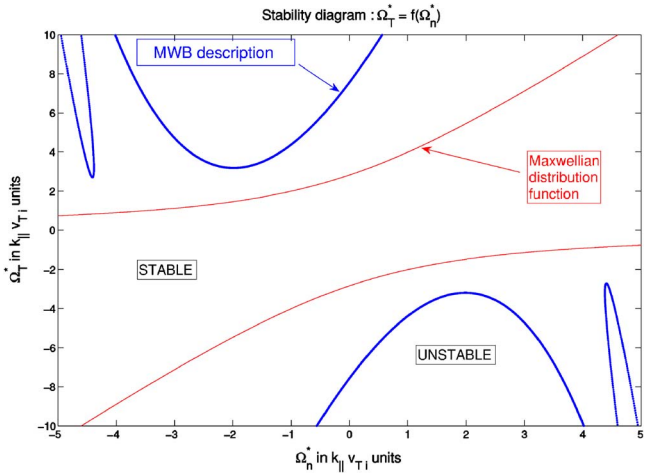

FIG. 7. (Color online) Dependence of $\Omega_T^\star$ on $\Omega_n^\star$ at the threshold for $N=3$, $a_N=3v_{Ti}$.

$$\epsilon_{k_\theta}(\omega) = 0,$$
$$d_\omega \epsilon_{k_\theta}(\omega) = 0. \tag{51}$$

A parametric approach relative to ω provides us a linear stability threshold.[43] Therefore, it is possible to compare these curves with an analytical result given in Ref. 10 in the case of a Maxwellian continuous distribution function (Figs. 7 and 8). In the three-bag case, we obtain two domains of existence of instabilities, with a lobelike structure (Fig. 7). Although a quantitative agreement is hard to obtain with such a small number of bags, actually, the qualitative features of ITG instability threshold are recovered.

The accuracy of the water-bag model improves rapidly with an increasing number of bags. Indeed, analyzing the dependence of the linear growth rate γ on the bag number N for $A(\Omega_n=-1.0, \Omega_T=-8.0)$ (see Fig. 8) close to the threshold shows that γ reaches, respectively, 93% and 98.5% of its continuous rate $(N\to\infty)$ for $N=5$ and $N=10$. This result

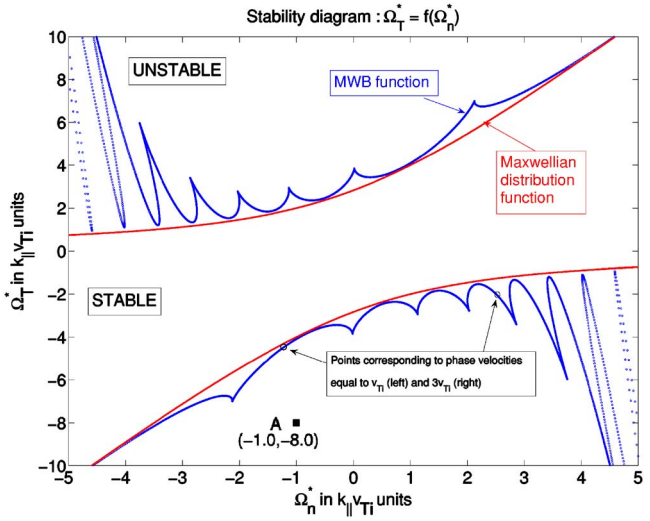

FIG. 8. (Color online) Dependence of $\Omega_T^\star$ on $\Omega_n^\star$ at the threshold for $N=10$, $a_N=5v_{Ti}$.

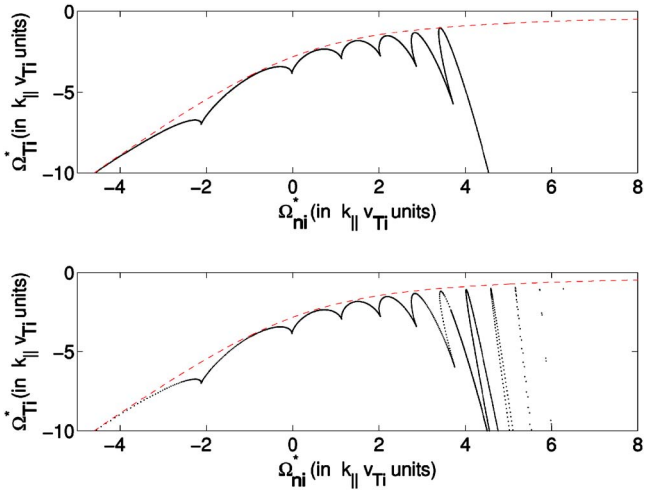

FIG. 9. (Color online) Dependence of the linear threshold on the value of a_N. With the parameters $Z_i^\star=1$, $N_{\text{top}}=8$, $a_8=15/19\times5v_{Ti}=3.95v_{Ti}$, $N_{\text{bottom}}=16$, $a_{16}=31/19\times5v_{Ti}=8.16v_{Ti}$, and $\Delta a=\text{const}=10/19=0.53$.

seems to suggest that for such usual coordinates (Ω_n,Ω_T) (see Refs. 10 and 42) about ten bags are enough to correctly describe ITG instabilities.

C. Influence of the water-bag parameters

With respect with our normalizations, increasing ω is the same as considering an increasing value of the phase velocity. As shown in Fig. 8 (see points associated with $\omega=v_{Ti}$ or $3v_{Ti}$), the large values of the phase velocity are located on the first and third quadrants, while the slow ones are located on the second and fourth ones.

We have drawn in Fig. 9 stability domains associated with $N=8$ and $N=16$ bags. We choose to deal with a constant interval Δa between each a_j, with the reference that the tenth bag contour a_{10} is located at five thermal velocities.

As shown in Fig. 9, by adding to the eight-bag case eight new bags, eight new lobes should occur and describe the fast phase velocities. However, the last ones do not appear on the figure because they are too thin; this phenomenon is clearly related to the very small value of the distribution function corresponding to those fast velocities. Accordingly, in the following, a cutoff velocity equal to five thermal velocities will be chosen, whatever the number of bags.

To describe ITG instabilities, the η parameter ($\eta=\Omega_T^\star/\Omega_n^\star$) is widely used. We can see in Fig. 9 that particles with velocities less than the thermal one are located near the $\eta=2$ asymptote, and fast particles generate the $\eta\to0$ asymptote.

D. The fluid limit

Going back to the dispersion equation, we can recover gyro fluid results by assuming small parallel wave number. If we consider unnormalized quantities, we have in this limit $\omega\gg k_\parallel v_{Ti}$. With our normalizations [Eq. (31)], such an approximation allows us to neglect the coupling between a bag and all others:

$$\frac{1}{\omega^2-a_j^2}\simeq\frac{1}{\omega^2}\left[1+\frac{a_j^2}{\omega^2}+o\left(\frac{a_j^4}{\omega^4}\right)\right], \tag{52}$$

where we have taken into account the small parameter $1/\omega^2\propto\epsilon^2$. The dielectric function (30) reads in that case

$$\epsilon_{k_\theta}(\omega)\simeq1-Z_i^\star\sum_{j=1}^{N}\alpha_j\frac{1-\omega\Omega_j^\star}{\omega^2}\left[1+\frac{a_j^2}{\omega^2}+o\left(\frac{a_j^4}{\omega^4}\right)\right]. \tag{53}$$

By considering only the two main terms, and using the relation $\Sigma_{j=1}^N\alpha_j\omega_j^\star=\Omega_n^\star$,

$$\omega=-Z_i^\star\Omega_n^\star, \tag{54}$$

we recover the basic result given by the fluid description; namely, the plasma response is an oscillation at the diamagnetic frequency $\omega_n^\star=-Z_i^\star\Omega_n^\star$. It is important to note that all other solutions are negligible with respect to the order in ω we consider.

By taking into account the two following terms, we have

$$\omega^3+Z_i^\star\Omega_n^\star\omega^2-Z_i^\star\omega+Z_i^\star(\Omega_n^\star+\Omega_T^\star)=0, \tag{55}$$

where we have used the momenta equivalence to explicit summations in terms of $\Omega_T^\star$ and $\Omega_n^\star$.

As compared with Eq. (54), Eq. (55) is an expansion with the following ordering:

$$\omega\sim\epsilon^{x-1},\qquad \Omega_X^\star\sim\epsilon^{-1}. \tag{56}$$

To obtain the limit $\omega\gg k_\parallel v_{Ti}$, it must be supposed that $x<1$.

With the assumption of a flat density profile, an analytical expression of the linear growth rate is obtained to the first order:

$$\gamma=\frac{\sqrt{3}}{2}|Z_i^\star\Omega_T^\star|^{1/3}. \tag{57}$$

The real part associated is of the same order in ϵ, and we validate $x=2/3<1$. Such a result is well known in the case of a Maxwellian distribution function (see, for example, Ref. 10).

The case of one bag recovers the result of a collisionless fluid description:

$$\omega^2+Z_i^\star\Omega_n^\star\omega-a_1^2-Z_i^\star\alpha_1=0. \tag{58}$$

Using the momenta definitions, we obtain the following:

$$\omega^2+Z_i^\star\Omega_n^\star\omega-(3+Z_i^\star)=0 \tag{59}$$

with the condition $\Omega_T^\star=2\Omega_n^\star$, which can also be expressed as $\eta=2$.

Therefore, a well known result is recovered: a collisionless fluid description is unable to describe any linear instability. The case of a flat density profile allows ion acoustic modes.

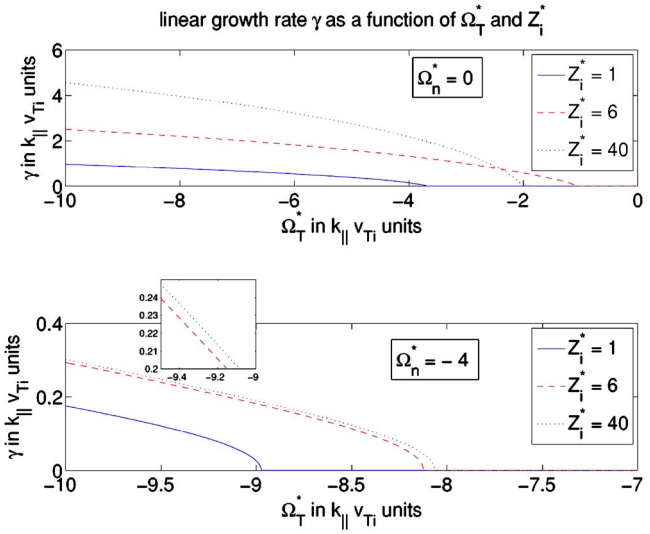

FIG. 10. (Color online) Influence of the Z_i^* parameter value on linear growth rate γ for two fixed values of density gradient $\Omega_n^\star$. $N=10$, $a_{\max}=5v_{Ti}$.

E. $Z_i^\star$ parameter and kinetic description

In the case of ion acoustic modes, kinetic effects are controlled in amplitude by the ion charge and the temperature ratio between electrons and ions. It follows that the $Z_i^\star = Z_i T_e / T_i$ parameter determines the amplitude of the kinetic Landau damping.[38] We investigate in the present section its effect on the competition between kinetic and fluid effects, particularly on relative values of the linear growth rate γ (see Fig. 10).

With an increasing value of $Z_i^\star$, and whatever the value of $\Omega_n^\star$, we can see in Fig. 10 that the linear growth rate increases globally.[44]

Another interesting feature of our model is to show that the linear growth rate of instability is maximal around the $\Omega_n^\star=0$ value, which corresponds to a flat density profile. The fact that the linear growth rate decreases as $\Omega_n^\star$ increases corresponds to the stabilizing effect of a density peaking. Such an effect is stronger for high values of $Z_i^\star$, as we can see on the bottom of Fig. 10, where the value of the linear growth rate γ is quite the same for $Z_i^\star=6$ or $Z_i^\star=40$.

We can conclude that the stabilizing effect of a density peaking increases with the $Z_i^\star$ value of the plasma (only composed of one ion population, with the assumptions of a cylindrical plasma column).

V. NONLINEAR WATER-BAG SIMULATION

The above results have been analytically obtained in the frame of a linear theory. How nonlinear effects modify the linear prediction is a question for which one needs to resort to numerical simulation. As compared to a fully gyrokinetic code, the water bag needs to cope only for a limited number of phase space trajectories (the contours) and it has been shown that typically ten bags could do the job at a reasonable price. It is beyond the scope of this paper to develop a full nonlinear water-bag code. We will present in the following the premises of this work.

In a seminal paper by Berk and Roberts,[27] each contour (and, more precisely, a phase space region in a neighborhood of the contour) was approximated by a chain of Lagrangian points. These points satisfy the particle equations of motion and at first glance it might appear that the problem of solving Vlasov's equation by computing the motion of these points should be similar to that of moving individual particles in a particle code.

However, this Lagrangian numerical scheme makes the computation of the contours difficult due to numerical noise inherent to particle model. An alternative method of following the evolution of the system is to track each contour C_j using now an Eulerian description; i.e., by solving the partial differential equation (3) with an Eulerian numerical scheme. Once the boundary curves are known, the distribution is well determined and it is not necessary to follow fluid points inside the regions even though they may be undergoing complicated motions.

To test the numerical ability of the water-bag model in solving nonlinear problems, the first step is to validate an appropriate numerical scheme in a simplified space. In the following, we present in the first section the nonlinear set of water-bag equations; the second part describes the discontinuous Galerkin (DG) method, a test of the solver in the case of Landau damping is achieved as an illustration.

A. The model

In this section, we consider an initial value problem with periodic boundary conditions

$$\partial_t v_j^\pm + v_j^\pm \partial_z v_j^\pm + \partial_z \phi = 0 v_j^\pm(0,\cdot) = v_{0j}^\pm(\cdot), \tag{60}$$

$$\phi = \frac{Z_i^\star}{n_{e0}}\left[Z_i \sum_{j=1}^{N} A_j (v_j^+ - v_j^-) - n_{e0}\right], \quad z \in \Omega = \,]0,L[. \tag{61}$$

We assume adiabatic electrons, with $\phi \ll 1$ (where ϕ is normalized to $\hat{\phi}=Z_i e\phi/T_i$), and we neglect any transverse dependency ($\Omega_T^\star=0, \Omega_n^\star=0$). The $Z_i^\star$ parameter represents the ion charge corrected by the temperature ratio, i.e., $Z_i^\star = Z_i T_e / T_i$; it controls the amplitude of the damping.

B. Description of the numerical method

In this section we present briefly the numerical method we use to solve Eqs. (60) and (61). The discontinuous Galerkin (DG) method[45,46] has been used to investigate these equations. This is a finite element method space discretization by discontinuous approximations, that incorporates the ideas of numerical fluxes and slope limiters used in high-order finite difference and finite volume schemes. The DG methods can be combined with Runge-Kutta or Lax-Wendroff time discretization scheme to give stable, high-order accurate, highly parallelizable schemes that can easily handle h-p adaptivity, complicated geometries, and boundaries conditions.

Let Ω be the domain of computation and $\mathcal{M}_h$ a partition of Ω of elements K such that $\cup_{K\in\mathcal{M}_h}\bar{K}=\bar{\Omega}$, $K\cap Q=\emptyset$, $K, Q \in \mathcal{M}_h$, $K\neq Q$. We set $h=\max_{K\in\mathcal{M}_h} h_K$, where h_K is the exterior diameter of a finite element K. The first step of the

method is to write Eq. (60) in a variational form on any element K of the partition $\mathcal{M}_h$. Using a Green formula, for all test-functions φ, for all $j=1,\ldots,N$, we get

$$\int_K \partial_t v_j^{\pm}\varphi - \int_K [\mathcal{F}(v_j^{\pm}) + \phi(z)]\partial_z\varphi dz + \int_{\partial K} [\mathcal{F}(v_j^{\pm}) + \phi(z)]n_K\varphi d\Gamma, \quad \forall\, K \in \mathcal{M}_h, \tag{62}$$

where ∂K denotes the boundary of K, n_K denotes the outward unit normal to ∂K, and $\mathcal{F}(\cdot)=(\cdot)^2/2$. Now we seek an approximate solution $(v_{h,j}^{\pm},\phi_h)$ whose restriction to the element K of the partition $\mathcal{M}_h$ of Ω belongs, for each value of the time variable, to the finite dimensional local space $\mathcal{P}(K)$, typically a space of polynomials. We now determine the approximate solution $(v_{h,j}^{\pm},\phi_h)_{|K} \in \mathcal{P}(K)\otimes\mathcal{P}(K)$ for $t>0$, on each element K of $\mathcal{M}_h$ by imposing that, for all $\varphi_h \in \mathcal{P}(K)$, for all $j=1,\ldots,N$,

$$\int_K \partial_t v_{h,j}^{\pm}\varphi_h - \int_K [\mathcal{F}(v_{h,j}^{\pm}) + \phi_h(z)]\partial_z\varphi_h dz + \int_{\partial K} [\widehat{\mathcal{F}n_K}(v_{h,j}^{\pm}) + \widehat{\phi_h n_K}]\varphi_h d\Gamma, \tag{63}$$

where we have replaced the flux terms $[\mathcal{F}(v_j^{\pm})+\phi]n_K$ in Eq. (62) by the numerical flux $\widehat{\mathcal{F}n_K}(v_{h,j}^{\pm})+\widehat{\phi n_K}$ because in Eq. (62), the terms arising from the boundary of the cell K are not well defined or have no sense since $v_{h,j}^{\pm}$, ϕ_h, and φ_h are discontinuous (by construction of the space of approximation) on the boundary ∂K of the element K. Now it remains to define the numerical flux $\widehat{\ }$. For two adjacent cells K^r and K^l (where r denotes the right cell and l the left one) of $\mathcal{M}_h$ and a point z of their common boundary at which the vector n_{K^α} with $\alpha \in \{r,l\}$ are defined, we set $\varphi_h^{\alpha}(z)=\lim_{\epsilon\to 0}\varphi_h(z-\epsilon n_{K^\alpha})$, and call these values the traces of φ_h from the interior of K^α. Therefore, the numerical flux at z is a function of the traces $v_{h,j}^{\pm,\alpha}$; i.e.,

$$\widehat{\mathcal{F}n_{K^l}}(v_{h,j}^{\pm})(z) = \widehat{\mathcal{F}n_{K^l}}\left(v_{h,j}^{\pm,l}(z), v_{h,j}^{\pm,r}(z)\right).$$

In addition, the numerical flux must be consistent with the nonlinearity $\mathcal{F}n_{K^l}$, which means that we should have $\widehat{\mathcal{F}n_{K^l}}(v,v)=\mathcal{F}(v)n_{K^l}$. In order to give a monotonic scheme in the case of piecewise-constant approximation, the numerical flux must be conservative; i.e.,

$$\widehat{\mathcal{F}n_{K^l}}\left(v_{h,j}^{\pm,l}(z), v_{h,j}^{\pm,r}(z)\right) + \widehat{\mathcal{F}n_{K^r}}\left(v_{h,j}^{\pm,r}(z), v_{h,j}^{\pm,l}(z)\right) = 0$$

and the mapping $v \mapsto \widehat{\mathcal{F}n_{K^l}}(v,\cdot)$ must be nondecreasing. There exist several examples of numerical fluxes satisfying the above requirements: the Godunov flux, the Engquist-Osher flux, and the Lax-Friedrichs flux (see Ref. 45). For the numerical flux $\widehat{\phi_h n_{K^l}}$ we can choose average, left, or right flux. We can also choose other numerical fluxes.[45,46] Therefore, for each cell K, after the space-discretization step, we get the ordinary differential equation (ODE)

$$\mathcal{M}\frac{d}{dt}v_{h,j|_K}^{\pm} = \mathcal{L}_K(\{v_{h,j|_{K'}}^{\pm}, \phi_{h|_{K'}} | \bar{K}' \cap \bar{K} \in \partial K\}), \quad \forall\, K \in \mathcal{M}_h, \quad j=1\ldots,N. \tag{64}$$

In the general case, the local mass matrix $\mathcal{M}$ of low order [equal to the dimension of the local space $\mathcal{P}(K)$] is easily invertible (if we choose orthogonal polynomials $\mathcal{M}$ as diagonal). Therefore, we have to solve the ODE

$$\frac{d}{dt}v_{h,j}^{\pm} = \mathcal{L}_h(v_{h,j}^{\pm},\phi_h), \quad j=1,\ldots,N. \tag{65}$$

In order to solve Eq. (65), we can use Runge-Kutta methods.[47] For the discretization of the initial condition, we take $v_{h,j}^{\pm}(0)$ on the cell K to be the L^2-projection of $v_{0h,j}^{\pm}(\cdot)$ on $\mathcal{P}(K)$; i.e., for all $\varphi_h \in \mathcal{P}(K)$,

$$\int_K v_{h,j}^{\pm}(0)\varphi_h dz = \int_K v_{0h,j}^{\pm}\varphi_h dz.$$

To solve Eq. (61), we take its L^2-projection on $\mathcal{P}(K)$; i.e., for all $\varphi_h \in \mathcal{P}(K)$,

$$\int_K \phi_h\varphi_h dz = \int_K \varphi_h \frac{Z_i^{\star}}{n_0}\left(Z_i\sum_{j=1}^{M} A_j(v_{h,j}^{+} - v_{h,j}^{-}) - n_0\right)dz.$$

C. Nonlinear Landau damping of ion acoustic waves

If a wave has a slow enough phase velocity to match the thermal velocity of ions, ion Landau damping can occur. The dispersion relation for ion wave is

$$\omega = (Z_i^{\star}+3)^{1/2}.$$

If $T_e \leqslant T_i$ or $T_e \sim T_i$, the phase velocity lies in the region where the Maxwellian unperturbed part of distribution function has a negative slope. Consequently, ion waves are heavily Landau damped. Ion waves propagate without damping if $T_e \gg T_i$, so that the phase velocity lies far in the tail of the ion velocity distribution. For a single ion species, for $k^2\lambda_D \ll 1$ (λ_D the Debye length) is

$$\mathcal{Z}'(\omega) = \frac{2T_i}{Z_i T_e} = \frac{2}{Z_i^{\star}},$$

where $\mathcal{Z}(\cdot)$ stands for the plasma dispersion function. The numeric value of the parameters are $L=4\pi$, $v_{\text{th}}=1$, $N=16$, $v_{\max}=6$, $n_0=1$, and $T_i/T_e=0.5$. The damping rate given by the numerical solution of the system (60) and (61) is $\gamma=-0.288$, which is in good agreement with the theoretical value $\gamma=-0.290$. Moreover, the theoretical normalized recurrence time $T_R=2\pi/(\Delta v)$ is equal to 32.46, which is in agreement with that observed in Fig. 11.

VI. DISCUSSION

The water-bag model appears to be an interesting alternative to the usual gyrokinetic description of a tokamak plasma. Interesting results have been obtained pointing to the ability of the gyro water bag to depict and resolve kinetic effects in the nonlinear regime.

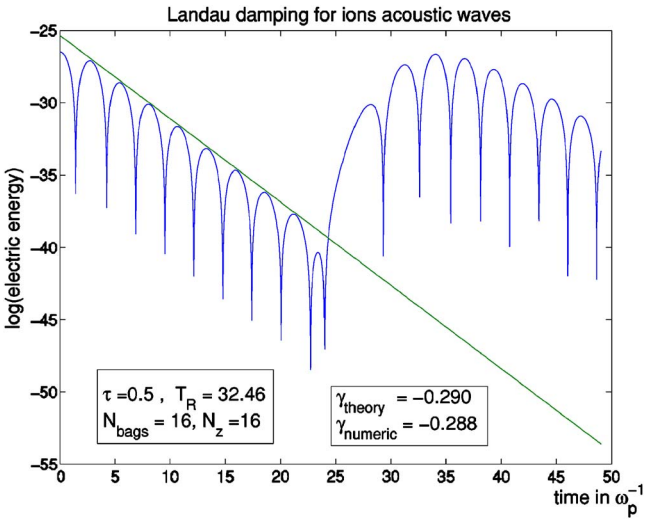

FIG. 11. (Color online) Evolution in time of the Logarithm of electric energy.

An original method has been developed to obtain satisfactory agreement with a continuous distribution function. More particularly, the momenta equivalence between continuous and multi-water-bag distribution functions allows us to obtain the relevant physical water-bag parameters.

The analytical formulation of the linear dispersion equation as a summation over an assembly of oscillators provides a very clear description of the Landau damping mechanism. Converting analytical problems into algebraic ones, without a loss of generality, represents one interesting property of the multi-water-bag model. As a direct consequence, the multi-water-bag problem converts the parallel velocity dependence into a set of contour equations.

Thus, the multiple water bag offers an exact description of the plasma dynamics even with a small bag number, in the sense that the water-bag concept makes full use of the Liouville invariance in phase space. From a physical point of view, many interesting results can be obtained even with a small N, sometimes $N=2$ or 3 allowing much more analytical approaches, bringing the link between the hydrodynamic description and the full Vlasov one.

However, if we need a precise description of a continuous distribution, it is clear that a larger N is needed; but even if the numerical effort is close to a standard discretization of the velocity space using equivalently $2N+1$ mesh points, the use of an exact water-bag sampling should give better results than approximating the corresponding differential operator.

Furthermore, there is no constraint on the shape of the distribution function which can be very far from a Maxwellian. In this paper we first wanted to test the water-bag approach for a case where analytical results are known. Hence, the choice of ITG modes for a Maxwellian plasma in a cylinder for which the linear stability is well known.

As an example, ITG linear modes are well described even with a ten-bag model: we obtained a good agreement between a water-bag distribution and a Maxwellian one.

Nonlinear simulations have been investigated preliminary in 2-D space case, the Landau damping rate recover its usual value. The Galerkin discontinuous numerical scheme provides an interesting solution for nonlinear multi-water-bag simulations.

Furthermore, finite Larmor radius (FLR) effects, which have been neglected in the present paper, are now under consideration without any further conceptual difficulties, and will be published in a forthcoming paper. It is important to point out that the water-bag concept (i.e., phase space conservation) is not affected by adding FLR or curvature terms, excepting of course a more complicated algebra.

For example, gyroaveraging and polarization drift effects have now been introduced using a cylindrical geometry. The presence of impurities in a plasma also strongly aspects its stability, and the water-bag model could describe easily the coupling between two ion populations. Finally, toroidal geometry, poloidal magnetic field and curvature effects are going to be implemented [Eqs. (1)–(6)], in order to simulate a toroidal ion turbulence in a tokamak, without any further conceptual difficulties as said before.

Nevertheless, collisions will not be taken into account due to phase space conservation properties required for using a water-bag description. However, within the aim of modeling collisions, appropriate equations for the A_j values have to be established. Analytical work on this fundamental topic is now under consideration.

[1] R. E. Waltz, Phys. Fluids **31**, 1962 (1988).
[2] H. Nordman, J. Weiland, and A. Jarmén, Nucl. Fusion **30**, 983 (1990).
[3] W. Dorland and G. W. Hammett, Phys. Fluids B **5**, 812 (1993).
[4] X. Garbet and R. E. Waltz, Phys. Plasmas **3**, 1898 (1996).
[5] G. Manfredi and M. Ottaviani, Phys. Rev. Lett. **79**, 4190 (1997).
[6] S. E. Parker, W. W. Lee, and R. A. Santoro, Phys. Rev. Lett. **71**, 2042 (1993).
[7] R. D. Sydora, V. K. Decyk, and J. M. Dawson, Plasma Phys. Controlled Fusion **38**, A281 (1996).
[8] Z. Lin, T. S. Hahm, W. W. Lee, W. M. Tang, and R. B. White, Phys. Plasmas **7**, 1857 (2000).
[9] G. Depret, X. Garbet, P. Bertrand, and A. Ghizzo, Plasma Phys. Controlled Fusion **42**, 949 (2000).
[10] V. Grandgirard, M. Brunetti, P. Bertrand, N. Besse, X. Garbet, P. Ghendrih, G. Manfredi, Y. Sarazin, O. Sauter, E. Sonnendrücker, J. Vaclavik, and L. Villard, J. Comput. Phys. **217**, 395 (2006).
[11] W. Dorland, F. Jenko, M. Kotschenreuther, and B. N. Rogers, Phys. Rev. Lett. **85**, 5579 (2000).
[12] J. Candy and R. E. Waltz, J. Comput. Phys. **186**, 545 (2003).
[13] B. Coppi, M. N. Rosenbluth, and R. Z. Sagdeev, Phys. Fluids **10**, 582 (1967).
[14] W. Horton, D. Choi, and W. M. Tang, Phys. Fluids **24**, 1077 (1981).
[15] F. Romanelli and S. Briguglio, Phys. Fluids B **2**, 754 (1990).
[16] A. M. Dimits, G. Bateman, M. A. Beer, B. I. Cohen, W. Dorland, G. W. Hammet, C. Kim, J. E. Kinsey, M. Kotschenreuter, A. H. Kritz, L. L. Lao, J. Mandrekas, W. M. Nevins, S. E. Parker, A. J. Redd, D. E. Shumaker, R. Sydora, and J. Weiland, Phys. Plasmas **7**, 969 (2000).
[17] G. W. Hammett and F. W. Perkins, Phys. Rev. Lett. **64**, 3019 (1990).
[18] N. Mattor, Phys. Plasmas **6**, 1065 (1999).
[19] T. Passot and P. L. Sulem, Phys. Plasmas **10**, 3906 (2003).
[20] H. Sugama, T.-H. Watanabe, and W. Horton, Phys. Plasmas **10**, 726 (2003).
[21] H. Sugama, T.-H. Watanabe, and W. Horton, Phys. Plasmas **14**, 022502 (2007).
[22] Y. Sarazin, V. Grandgirard, E. Fleurence, X. Garbet, Ph. Ghendrih, P. Bertrand, and G. Depret, Plasma Phys. Controlled Fusion **47**, 1817 (2005).
[23] D. C. DePackh, J. Electron. Control **13**, 417 (1962).
[24] M. R. Feix, F. Hohl, and L. D. Staton, *Nonlinear Effects in Plasmas*, edited by G. Kalmann and M. R. Feix (Gordon and Breach, New York, 1969), pp. 3–21

[25]P. Bertrand and M. R. Feix, Phys. Lett. **28A**, 68 (1968).
[26]P. Bertrand and M. R. Feix, Phys. Lett. **29A**, 489 (1969).
[27]H. L. Berk and K. V. Roberts, in *Methods in Computational Physics*, edited by B. Alder, S. Fernbach, and M. Rotenberg (Academic, New York, 1970), Vol. 9, p. 29.
[28]U. Finzi, Plasma Phys. **14**, 327 (1972).
[29]M. R. Feix, P. Bertrand, and A. Ghizzo, in *Advances in Kinetic Theory and Computing*, Series on Advances in Mathematics and Applied Science, edited by B. Perthame (World Scientific, Singapore, 1994), Vol. 22, pp. 42–82.
[30]M. Navet and P. Bertrand, Phys. Lett. **34A**, 117 (1971).
[31]P. Bertrand, Ph.D. thesis, Université de Nancy, France, 1972.
[32]P. Bertrand, J. P. Doremus, G. Baumann, and M. R. Feix, Phys. Fluids **15**, 1275 (1972).
[33]P. Bertrand, M. Gros, and G. Baumann, Phys. Fluids **19**, 1183 (1976).
[34]T. S. Hahm, Phys. Fluids **31**, 2670 (1988).
[35]M. Gros, P. Bertrand, and M. R. Feix, Plasma Phys. **20**, 1075 (1978).
[36]N. G. Van Kampen, Physica (Amsterdam) **21**, 959 (1955).
[37]K. M. Case, Ann. Phys. **7**, 349 (1959).
[38]F. F. Chen, *Introduction to Plasma Physics and Controlled Fusion* (Plenum, New York, 1984), Vol. 1, pp. 271–272.
[39]G. Manfredi, Phys. Rev. Lett. **79**, 2815 (1997).
[40]P. Morel, E. Gravier, N. Besse, and P. Bertrand, Commun. Nonlinear Sci. Numer. Simul. **13**, 11 (2008).
[41]T. Dannert and F. Jenko, Phys. Plasmas **12**, 072309 (2005).
[42]Y. Sarazin, V. Grandgirard, G. Dif-Pradalier, X. Garbet, and Ph. Ghendrih, Phys. Plasmas **13**, 092307 (2006).
[43]P. Morel, E. Gravier, N. Besse, and P. Bertrand, in 33rd EPS Conference on Plasma Physics, Rome, 19–23 June 2006, Europhys. Conf. Abstr. Vol. 301, P-4.162.
[44]C. Bourdelle, "Analyse de stabilité de plasmas de Tokamak," Ph.D. thesis, Université Joseph Fourier-Grenoble 1, 2000.
[45]B. Cockburn and C.-W. Shu, J. Sci. Comput. **16**, 173 (2001).
[46]N. A. Douglas, F. Brezzi, B. Cockburn, and D. Marini, SIAM (Soc. Ind. Appl. Math.) J. Numer. Anal. **39**, 1749 (2002).
[47]S. Gottlieb, C.-W. Shu, and E. Tadmor, SIAM Rev. **43**, 89 (2001).